



OPEN ACCESS

EDITED BY

François Fournier,
Aix-Marseille Université, France

REVIEWED BY

Jinmin Song,
Chengdu University of Technology, China
Subhobroto Mazumder,
Oil and Natural Gas Corporation, India

*CORRESPONDENCE

Qinyu Xia,
✉ xiaqy-ordos@petrochina.com.cn

RECEIVED 08 May 2024

ACCEPTED 30 December 2024

PUBLISHED 30 January 2025

CITATION

Xia Q, Guo Z, Zhang F, Zhang L, Xu R, Wang X,
Li W, Shi S, Yan H and Liu Y (2025) Sedimentary
architecture of the microbial mound–shoal
complex: a case study of the Ediacaran
Dengying Formation, Sichuan Basin, China.
Front. Earth Sci. 12:1429584.
doi: 10.3389/feart.2024.1429584

COPYRIGHT

© 2025 Xia, Guo, Zhang, Zhang, Xu, Wang, Li,
Shi, Yan and Liu. This is an open-access article
distributed under the terms of the [Creative
Commons Attribution License \(CC BY\)](#). The
use, distribution or reproduction in other
forums is permitted, provided the original
author(s) and the copyright owner(s) are
credited and that the original publication in
this journal is cited, in accordance with
accepted academic practice. No use,
distribution or reproduction is permitted
which does not comply with these terms.

Sedimentary architecture of the microbial mound–shoal complex: a case study of the Ediacaran Dengying Formation, Sichuan Basin, China

Qinyu Xia^{1*}, Zhenhua Guo¹, Fei Zhang², Lin Zhang¹, Rui Xu²,
Xue Wang¹, Wenzheng Li¹, Shuyuan Shi¹, Haijun Yan¹ and
Yuyang Liu¹

¹Research Institute of Petroleum Exploration and Development, Petro China, Beijing, China,

²Southwest Oilfield Company, Petro China, Chengdu, China

The Ediacaran Dengying Formation in the Sichuan Basin exhibits well-developed microbial mound–shoal complex (MMSC) sedimentation. Its abundant outcrops, core samples, and thin section data provide advantageous conditions for sedimentary architecture studies. Based on these data, this study elucidates typical lithofacies, identifies sedimentary architectural elements, summarizes MMSC stacking styles, describes sedimentary evolution characteristics, and explores the controlling factors of different stacking styles and the reservoir development conditions of architectural elements. Research indicates that MMSC primarily develops five lithofacies, namely, thrombolitic dolomite, undulate stromatolitic dolomite, laminar stromatolitic dolomite, granular dolomite, and micritic dolomite. MMSC sedimentary architecture is categorized into composite MMSCs, single MMSCs, and lithofacies. Three stacking styles of MMSCs are observed, namely, superimposed MMSCs, which represent aggradational sedimentation; migratory MMSCs, which depict progradational sedimentation; and isolated MMSCs, which denote a single parasequence depositional cycle. The stacking styles of MMSCs are fundamentally controlled by the relationship between MMSC sedimentation rates and variations in accommodation space, with the latter predominantly influenced by fluctuations in sea level. Superimposed MMSC sedimentation rates are comparable to accommodation space change rates, while migratory MMSC sedimentation rates exceed accommodation space change rates, and isolated MMSC sedimentation rates are lower than accommodation space change rates. Various composite MMSCs are isolated from each other by sediments formed under low hydrodynamic conditions, constituting distinct connectivity units. Compared to isolated MMSCs, superimposed and migratory MMSCs exhibit superior reservoir conditions. Within individual MMSCs, different lithofacies lead to high-quality reservoirs in mound cores and flanks due to variations in physical properties, while mound bases, flats, and caps form non-reservoirs.

KEYWORDS

microbial mound–shoal complex, sedimentary architecture, Ediacaran, Dengying formation, Sichuan basin

1 Introduction

Microbialite is a type of rock formed through the lithification of sediments created by microbial trapping, encrustation, or cementation of detrital grains or microbial mineralization (Burne and Moore, 1987; Riding, 1991; Riding, 2011). From Early Archean to Early Paleozoic times, microbialites flourished globally, with significant development in the Mesoproterozoic, Cambrian, and Ordovician periods (Dalrymple and James, 2010; Li et al., 2013; Luo P. et al., 2013). Microbialites are crucial hydrocarbon reservoirs, with discoveries in regions such as the Upper Jurassic Smackover Formation in the Gulf of Mexico (Mancini et al., 2004; Mancini et al., 2008; Mancini et al., 2000), the Precambrian–Cambrian of East Siberia in Russia (Tull, 1997), and the Lower Cambrian Xiaerbulake Formation of the Tarim Basin in China (Song et al., 2012). In recent years, significant exploration breakthroughs have been made in the Ediacaran Dengying Formation microbial carbonate reservoirs in the Sichuan Basin, where natural gas reserves exceed 10 trillion cubic meters (Tian et al., 2020; Yang et al., 2021; Xia et al., 2021; Xia et al., 2022). Some Dengying Formation gas fields have been successfully developed with excellent production outcomes, yielding over 6 billion cubic meters annually (Zhou et al., 2022; Dong et al., 2023; Xia et al., 2024).

Microbialite deposition predominantly comprises microbial mounds or microbial mound–shoal complexes (MMSCs), the latter of which have been extensively studied by scholars in Cambrian and Precambrian strata across multiple basins in China (Ren et al., 2023). Currently, scholars have conducted research on the composition (Riding, 2002; Bridges et al., 1995), formation mechanisms (Bathurst, 1982; Pratt, 1982; Reitner et al., 1995; Schlager, 2003), classification (Riding, 2002; Pas et al., 2011; Tosolini et al., 2012), and evolution (Bosence et al., 1995; Pratt et al., 1995; Krause et al., 2004) of microbial mounds. Previous research has delved deep into clastic rock sedimentary architectures and has also explored sedimentary architectures of reefs, shoals (Cai and Jia, 1995; Wang et al., 2021), and microbial buildups (Khanna et al., 2020). Nevertheless, research on the sedimentary architectural stacking styles, controlling factors, and their reservoir-controlling effects in MMSCs remains insufficient. In addition, MMSCs in the Dengying Formation have become a focal area of geological research and oil and gas exploration and development in the Sichuan Basin in recent years. However, the production dynamics of underground gas reservoirs indicate significant differences in controlled reserves and control radii among different gas wells, severe polarization in well production rates, and noticeable disparities in the utilization of reserves in different blocks. Although reservoirs are significantly affected by diagenesis, MMSCs remain the primary factors controlling the development of high-quality reservoirs and connectivity units. Therefore, a thorough analysis of the sedimentary architecture of MMSCs in the Dengying Formation is crucial for characterizing high-quality reservoirs and connectivity units in gas reservoirs, deploying infill wells, and enhancing the utilization of reserves.

Due to constraints imposed by the number of wells drilled and the resolution of seismic data, conducting research on MMSC sedimentary architecture using well logging and seismic data poses significant challenges. Analogous studies of subsurface reservoir architecture based on outcrops from the same geological

period and similar sedimentary environments are commonly employed and constitute a vital method in sedimentary architecture research. Outcrop analogs facilitate the provision of crucial information regarding the scale, morphology, and connectivity of subsurface geological bodies in a more convenient and intuitive manner (Howell et al., 2014). Consequently, they have garnered considerable scholarly attention since the 1960s. The Dengying Formation outcrops of the Sichuan Basin are abundant, with some outcrops displaying sedimentary backgrounds consistent with developed gas reservoirs, characterized by carbonate platforms featuring MMSC deposition rather than slopes or basins. Thus, these outcrops serve as excellent subjects for analog studies of sedimentary architecture. Specifically, the Xianfeng, Hujiaaba, and Yangba outcrops exhibit relatively favorable conditions for exposing the Dengying Formation. Moreover, these three locations represent different positions of MMSC deposition on the platform during the Dengying Formation period, each showing diverse characteristics in sedimentary architecture and stacking styles. Therefore, they are selected as research targets. Furthermore, since no outcrop perfectly matches underground reservoirs, conducting comprehensive analog studies across multiple outcrops and integrating and comparing geological information from different outcrops is essential.

Therefore, the objective of this study is to utilize outcrops of MMSCs from the Dengying Formation as analogs for subsurface gas reservoirs to conduct sedimentary architecture research. This involves integrating drilling core and thin section data to elucidate typical lithofacies, identify sedimentary architectural elements, summarize MMSC stacking styles, describe sedimentary evolution characteristics, and explore the controlling factors of different MMSC stacking styles and the reservoir development conditions of MMSC architectural elements. This study aims to provide geological evidence for characterizing high-quality reservoirs and connectivity units in underground gas reservoirs and serve as a reference for dissecting sedimentary architectures of similar carbonate sedimentary bodies.

2 Geological background

During the Ediacaran Period (635–539 Ma), global plate tectonics witnessed the Pan-African orogeny, leading to the fragmentation of the southern and northern Rodinia supercontinent and the amalgamation of the Congo craton into the megacontinent of Gondwana (also known as the Pannotia supercontinent). The Yangtze Block was situated in the northern part of Gondwana (Song et al., 2024) (Figure 1A). At approximately 560 Ma, Gondwana began to rift, resulting in the formation of Laurentia, Baltica, Siberia, and Gondwana continents (Scotese, 2009), with the Deyang–Anyue rift developing in the western part of the Yangtze Block (Wang et al., 2020) (Figure 1C).

The Sichuan Basin, located in Southwestern China (Figure 1B), is a large oil- and gas-bearing superimposed basin developed on the basement of the Yangtze Block. Based on lithological variations, the Dengying Formation in the Sichuan Basin is divided into four members from bottom to top (Xia et al., 2023) (Figure 1D), namely, Deng-1, Deng-2, Deng-3, and Deng-4. Deng-1 is characterized by a microbial-poor interval dominated by micritic dolomite, with a thickness of 200–300 m. Deng-2 consists of a microbial-rich interval

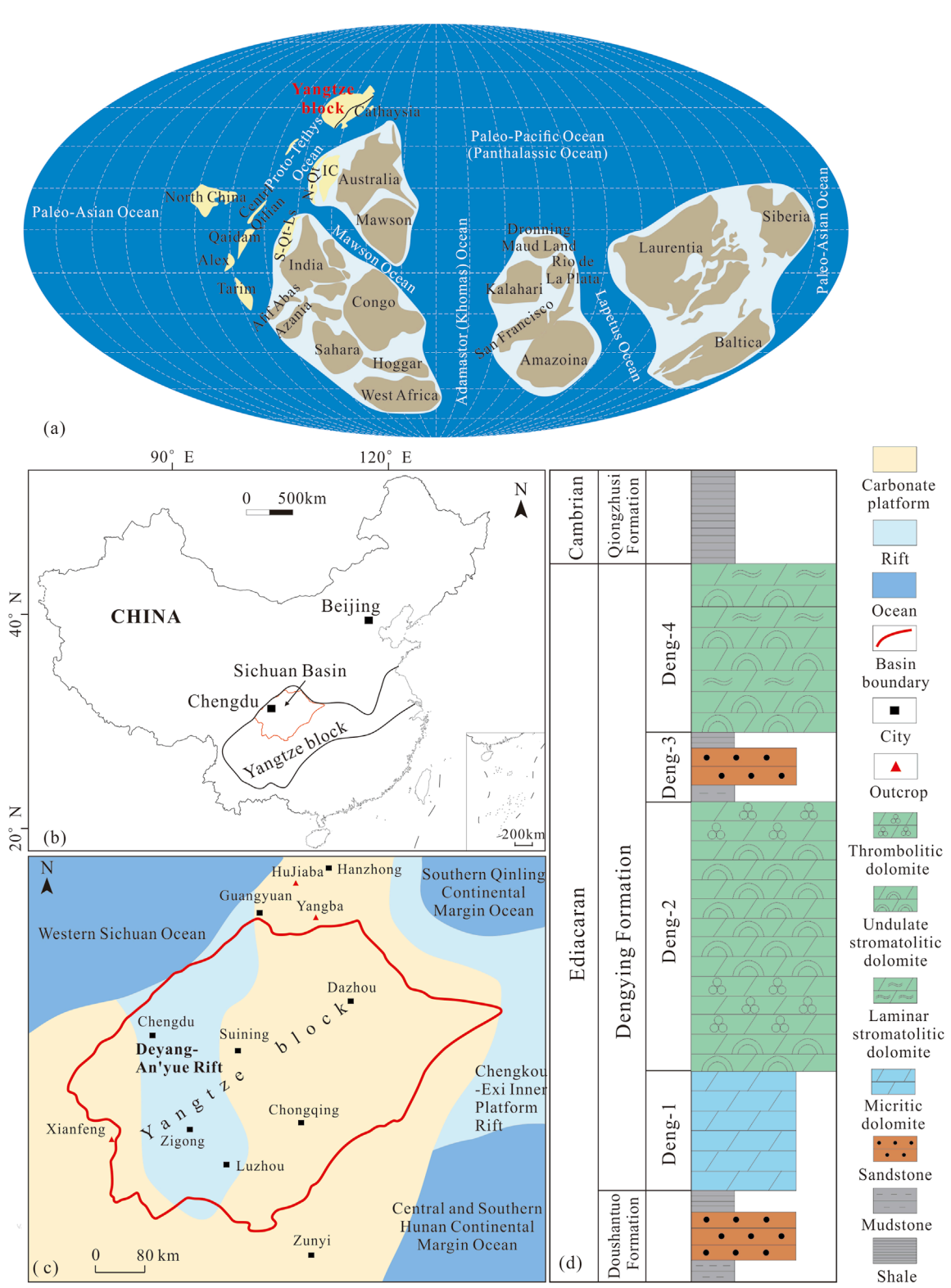
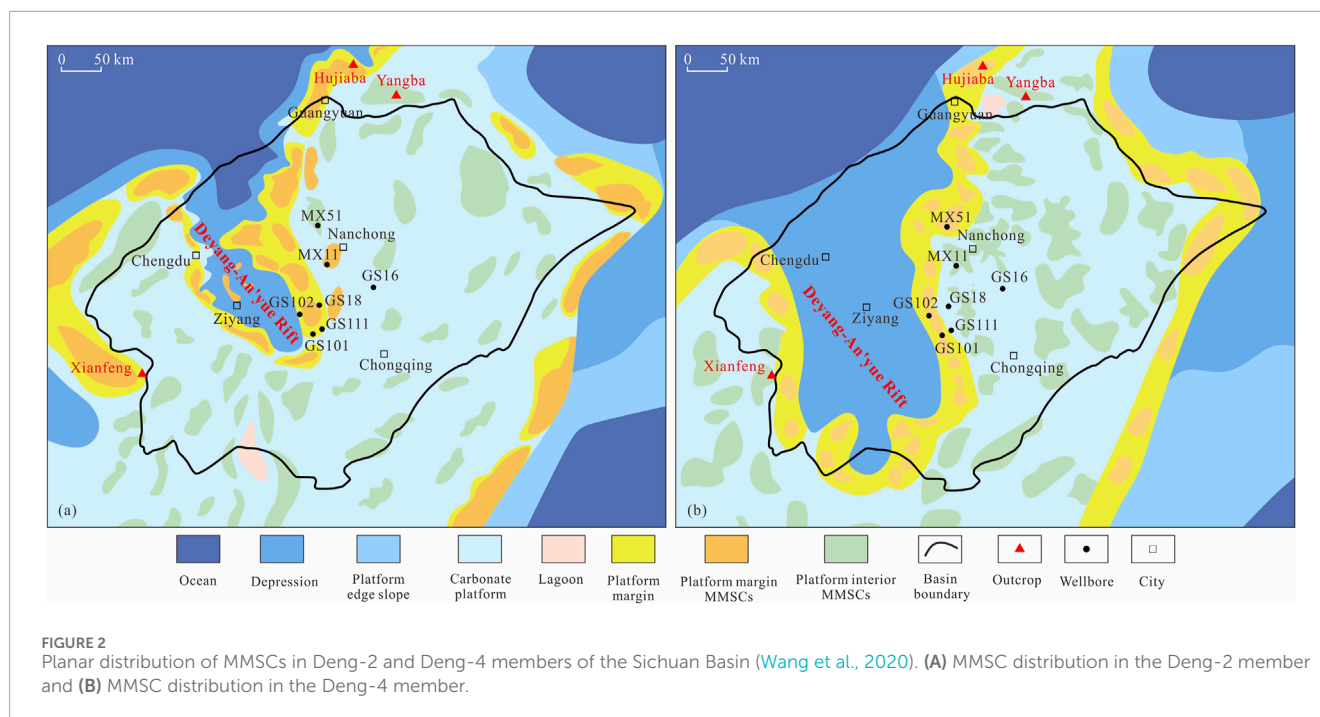


FIGURE 1 Tectonic setting and stratigraphic characteristics of the Sichuan Basin in the Ediacaran. (A) Location of the Yangtze Block in the Ediacaran (Song et al., 2024); (B) location of the Sichuan Basin in China; (C) Ediacaran tectonic setting in the Sichuan Basin (Wang et al., 2020); and (D) stratigraphy of the Dengying Formation.



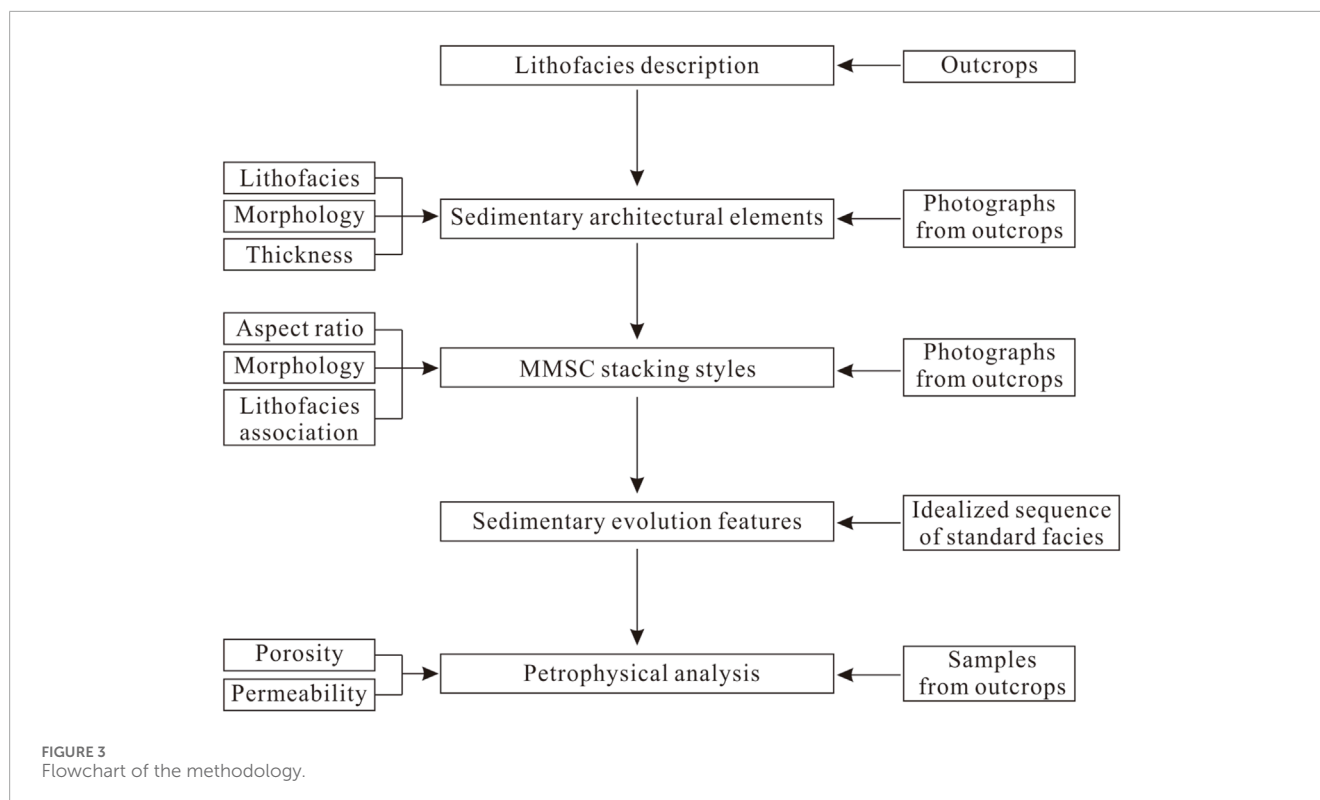
primarily composed of thrombolitic dolomite, with a thickness of 300–400 m. Deng-3 represents a microbial-poor interval, mainly composed of siltstone and argillaceous siltstone, with thinly bedded chert developing in the upper section. Its thickness ranges from 10 to 120 m. Deng-4 is a microbial-rich interval characterized by undulate stromatolitic dolomite, laminar stromatolitic dolomite, and locally developed thrombolitic dolomite, with a thickness ranging from 30 to 400 m (Zhao et al., 2022).

During the Dengying Formation deposition period, the Upper Yangtze Craton, situated in the low-latitude zone near the equator, experienced stable carbonate platform sedimentation. The climate was warm and conducive to prolific microbial growth, fostering favorable conditions for MMSC development (Ren et al., 2023). MMSCs primarily developed in the Deng-2 and Deng-4 members. Along the margins of the Deyang–Anyue rift, a carbonate platform margin developed where MMSC sedimentation was thick and widespread, while MMSCs were sporadically present within the platform interior (Wang et al., 2020) (Figure 2).

3 Materials and methods

The Ediacaran Dengying Formation outcrops abundantly in the Sichuan Basin, with favorable exposure conditions. Additionally, gas reservoirs within the basin's Dengying Formation have been actively developed, yielding rich drilling data. The outcrops exhibit sedimentary conditions comparable to those of the developed gas reservoirs in the basin. This abundance of data provides a solid foundation for lithofacies delineation, sedimentary architecture analysis, analysis of MMSC stacking styles, and the evolutionary characteristics of MMSC sedimentation (Figure 3). (1) This study utilized three field outcrops from the Xianfeng, Hujiaba, and Yangba areas, capturing photographs and describing five typical

sedimentary lithofacies of the Deng-2 and Deng-4 stages in these regions. Additionally, lithofacies analysis of MMSCs was conducted using core and thin section data from seven drilled wells within the basin (Figure 2). Thin sections were prepared by impregnating rocks with blue liquid epoxy, enhancing pore space visualization, and observed under a polarizing microscope (Nikon Eclipse E600 POL). Lithofacies were classified based on Dunham's carbonate rock classification system. (2) Macroscopic photographs of MMSCs from three outcrops were utilized to anatomize the sedimentary architectures of MMSCs. Detailed descriptions were provided regarding lithofacies characteristics, thickness variations, external morphology, and identification criteria of different sedimentary architectural elements. (3) Based on macro photographs of MMSCs captured at three outcrops, the stacking styles of MMSCs were summarized according to sedimentary architectural hierarchy, accompanied by descriptions of aspect ratios, external morphologies, sedimentary characteristics, and lithofacies associations of different MMSC stacking styles. (4) Detailed descriptions of lithofacies characteristics of the Deng-2 and Deng-4 members at three outcrops were also provided, along with an analysis of sedimentary evolution features. The analysis of sedimentary evolution characteristics was led by the idealized sequence of standard facies (Wilson, 1975). The platform margin division scheme was illustrated by the facies model of carbonate sedimentation on a shelf (Tucker, 1985). (5) A total of 86 samples from different MMSC sedimentary architectural elements, collected from three outcrops, were analyzed for petrophysical properties. Porosity and permeability measurements were conducted using an automated permeameter-porosimeter (AP-608, United States). All analyses were performed at the Analysis Experiment Center of the Exploration and Development Research Institute of PetroChina Southwest Oil and Gasfield Company.



4 Results

4.1 Lithofacies

Preliminary studies indicate that in the Sichuan Basin, the Ediacaran Dengying Formation has accumulated a suite of shallow-marine sedimentary materials (Wang et al., 2016). The lithofacies of MMSCs mainly include thrombolitic dolomite, undulate stromatolitic dolomite, laminar stromatolitic dolomite, granular dolomite, and micritic dolomite.

4.1.1 Thrombolitic dolomite

Macroscopically, thrombolitic dolomite exhibits a clotted texture, with dark-colored algal deposits forming sponge-like structures (Figure 4A). Light gray micritic dolomites occur between the clots (Figure 4B). Under the microscope, these clots aggregate into cluster-like assemblages. These microbial clusters further coalesce and intertwine, interconnecting to form a reticular framework with grid-like cavities internally filled or partially filled with calcsparite (Figure 4C). This indicates that thrombolites form under significant hydraulic conditions, thus categorizing this lithofacies as mound core sedimentation. Mound cores predominantly develop under conditions of decreasing sea levels and shallowing water bodies and are predominantly composed of rock types formed under high hydrodynamic conditions.

4.1.2 Undulate stromatolitic dolomite

Undulate stromatolitic dolomite exhibits distinct laminated texture under both hand specimens and microscopes, featuring alternating light and dark laminae (Figures 4D, E). The laminae

exhibit pronounced undulations, with a thickness ranging approximately from 0.3 to 0.8 mm. Microscopically, the laminae often display conspicuous localized deformation. Internally, the laminae are characterized by small lattice-like primary pores (Figure 4F), frequently filled with fine crystalline dolomite cement. The formation of stromatolites is closely tied to hydrodynamic conditions. Undulate stromatolites are products of moderate hydrodynamic conditions. Therefore, we interpret this lithofacies also as mound core deposition with strong hydrodynamics.

4.1.3 Laminar stromatolitic dolomite

Laminar stromatolitic dolomite on hand specimens exhibits overall flat to wavy laminae (Figures 4G, H), with good lateral continuity. Microscopically, boundaries between light and dark laminae often display low-amplitude undulations and locally exhibit gradational features (Figure 4I). Dark laminae are primarily composed of dark-colored microbial textures and micritic dolomites. Light laminae constitute the matrix, with slightly coarser crystalline grains, predominantly consisting of crystalline powder dolomite. These stromatolites display a flat distribution of laminae, indicating deposition in low hydrodynamic settings of relatively quiescent water, interpreted as mound base or mound flat deposits. Mound base developed during the early stages of MMSC sedimentation, characterized by weak hydrodynamics. Mound flats formed during rapid sea level fall, resulting in shallowing water and reduced accommodation space, with the upper MMSC exposed to tidal flat conditions. Both environments can give rise to laminar stromatolites.

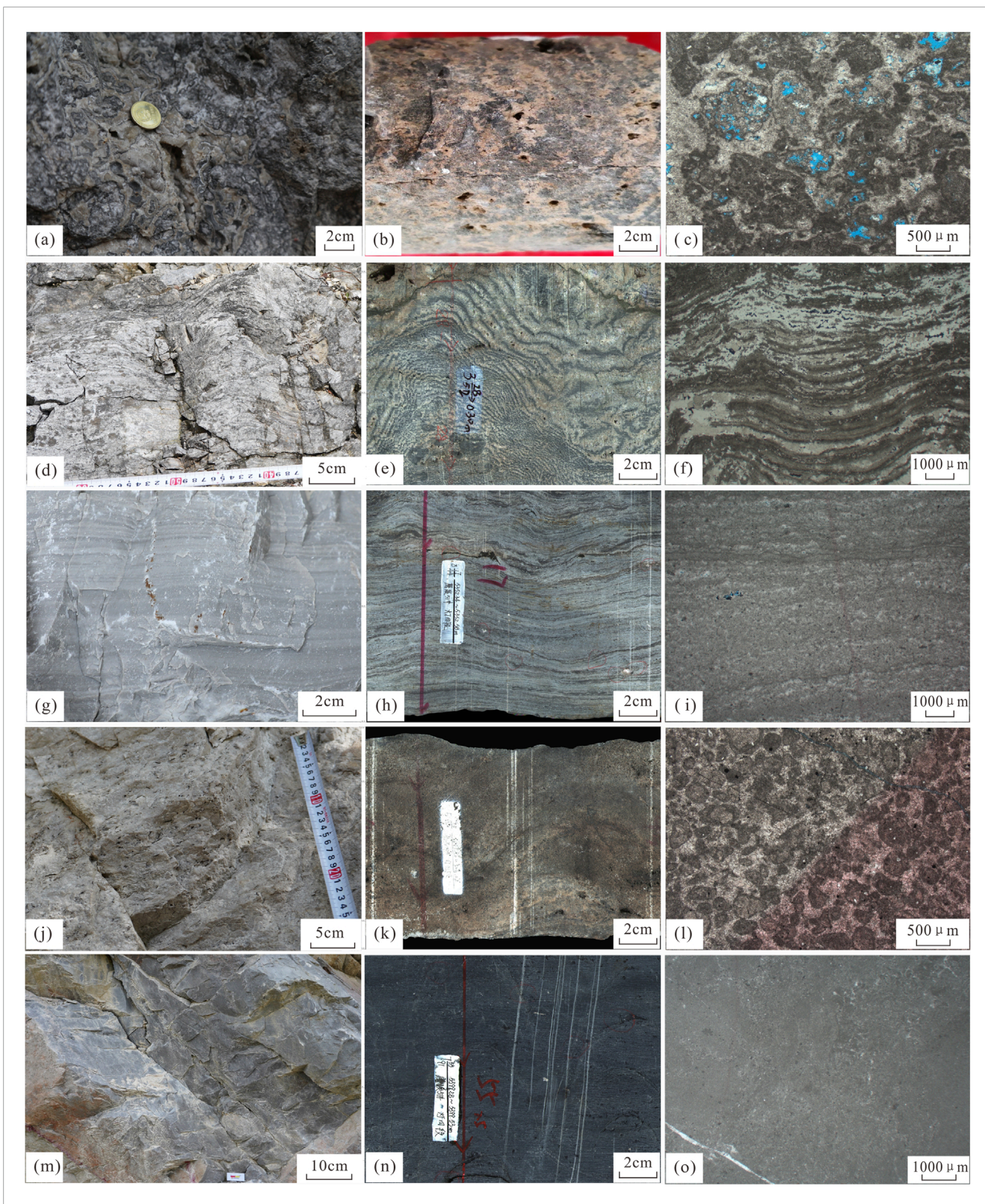


FIGURE 4 Typical lithofacies characteristics of MMSCs in the Dengying Formation, Sichuan Basin. **(A)** Thrombolitic dolomite, Xianfeng outcrop, Deng-2 member; **(B)** thrombolitic dolomite, core of the GS101 well, Deng-4 member; **(C)** thrombolitic dolomite, thin section of the GS18 well, Deng-4 member; **(D)** undulate stromatolitic dolomite, Hujiaba outcrop, Deng-2 member; **(E)** undulate stromatolitic dolomite, core of the GS111 well, Deng-4 member; **(F)** undulate stromatolitic dolomite, thin section of the GS18 well, Deng-4 member; **(G)** laminar stromatolitic dolomite, Xianfeng outcrop, Deng-2 member; **(H)** laminar stromatolitic dolomite, core of the MX51 well, Deng-4 member; **(I)** laminar stromatolitic dolomite, thin section of the MX11 well, Deng-4 member; **(J)** granular dolomite, Hujiaba outcrop, Deng-4 member; **(K)** granular dolomite, core of the GS102 well, Deng-4 member **(L)** granular dolomite, thin section of the GS16 well, Deng-4 member; **(M)** micritic dolomite, Hujiaba outcrop, Deng-2 member; **(N)** micritic dolomite, core of the MX51 well, Deng-4 member; and **(O)** micritic dolomite, thin section of the GS18 well, Deng-4 member.

4.1.4 Granular dolomite

Most of the grains in the granular dolomite are not directly in contact, presenting an overall floating appearance with distinct microbial encrustation features. The grains primarily consist of intraclasts (Figures 4J, K), predominantly derived from early formed microbial carbonates that were broken by waves and redeposited, showing microbial fabrics (Figure 4L). Microbial binding traces are visible between grains (Riding, 1991). Intergranular pores are predominantly filled with dolosparite, exhibiting well-developed dissolution porosity. We consider the granular dolomite to belong to the mound flank deposition. This lithofacies represents sedimentation near the wave base, where an early formed microbial mound was broken by waves, transported, and deposited on either side of the mound.

4.1.5 Micritic dolomite

Micritic dolomite appears gray–black to black, displaying horizontal bedding (Figure 4M). Macroscopically and under the microscope, microbial structures are not developed, with micrite predominating (Figures 4N, O). This lithofacies represents products of low hydrodynamic environments, classified as mound cap deposits or inter-mound deposits. During the late growth stage of MMSCs, rapid marine transgression occurred, leading to increased water depth. Sedimentation rates of MMSCs were slower than the rate of sea level rise, resulting in weakened hydrodynamics and cessation of MMSC growth.

4.2 Sedimentary architectural elements

Based on field outcrops of the Ediacaran Dengying Formation in the Sichuan Basin, a hierarchical analysis of MMSCs was conducted to delineate sedimentary architectural elements and describe their characteristics. This study categorizes MMSCs into composite MMSCs, single MMSCs, and lithofacies.

4.2.1 Composite MMSCs

Composite MMSCs are conglomerates formed by multiple solitary MMSCs within approximately the same period (Figure 5A). They consist primarily of thrombolitic, granular, and undulate stromatolitic dolomites, with minor amounts of micritic and laminar stromatolitic dolomites. These composite MMSCs exhibit significant vertical thicknesses, ranging up to 4–20 m, and typically display a flat bottom and convex top morphology. Different composite MMSCs are distinguished by the development of extensive sets of thick inter-mound deposits. Vertically, composite MMSCs can manifest as either single or combined repetitions of mound base, mound core, and mound flank or mound base, mound core, and mound flat associations.

4.2.2 Single MMSC

A single MMSC is comprised of various lithofacies, forming relatively independent units. They are primarily composed of thrombolitic and undulate stromatolitic dolomites, with minor amounts of laminar stromatolitic and granular dolomites. The vertical thickness of a single MMSC typically ranges from 1 to 10 m, predominantly falling within the 1–5 m range (Figure 5A). Apart from inter-mound deposits serving as distinguishing

markers between single MMSCs, variations in thickness, elevation differences, and the occurrence of mound flank sedimentation are observed. Vertically, single MMSCs can exhibit combinations of mound base–mound core–mound flat or mound base–mound core–mound cap configurations.

4.2.3 Lithofacies

The unit thickness at this level is limited, with the mound core composed predominantly of thrombolitic dolomites (Figure 5B), reaching thicknesses of over 5 m in some instances, while other unit configurations are thinner. The primary identification criteria for this unit configuration are lithological and morphological differences, with the mound core dominated by thrombolitic or undulate stromatolitic dolomites, situated in the central part of a single MMSC, presenting as medium-thick layers. The mound flanks are primarily composed of granular dolomites (Figure 5C), located on either side of the single MMSC, appearing as medium-thin wedge-shaped layers. The mound base or mound cap consists predominantly of laminar stromatolitic dolomites (Figure 5D), positioned, respectively, at the bottom and top of the single MMSC, both presenting as thin sheet-like layers.

4.3 MMSC stacking styles

In the Sichuan Basin, the Dengying Formation exhibits superimposed MMSCs, migratory MMSCs, and isolated MMSCs.

4.3.1 Superimposed MMSCs

The superimposed MMSCs exhibit a high uplift magnitude and large scale, with an overall width-to-height ratio ranging from 1 to 3. They present as thick block-like layers, representing vertical accretion of single MMSCs over multiple periods (Figure 6). Superimposed MMSCs manifest longitudinally as multiple phases of upward-shallowing sedimentary cycles, with each cycle corresponding to a single MMSC. The lower part of each sedimentary cycle consists of laminar stromatolitic dolomites transitioning upward into thrombolitic dolomites or undulate stromatolitic dolomites. The development of mound flats occurs at the top because of shallowing water bodies. As a result, the superimposed MMSCs exhibit a combination of mound base, mound core, and mound flat.

4.3.2 Migratory MMSCs

Migratory MMSCs exhibit moderate uplift amplitudes and scales, with an overall width-to-height ratio ranging from 3 to 10. They manifest as moderately thick tabular layers, characterized by the lateral accretion of single MMSCs over multiple periods (Figure 6). Migratory MMSCs display a series of upward-shallowing cycles. Typically, the lower portion consists of laminar stromatolitic dolomites, transitioning upward to thrombolitic, undulate stromatolitic, and granular dolomites. The overlapping position exhibits a combination of mound base, mound core, and mound flank.

4.3.3 Isolated MMSCs

Isolated MMSCs exhibit low uplift amplitude and small scale (Figure 6), with a width-to-height ratio greater than 10, presenting a thin sheet-like appearance. The isolated MMSC

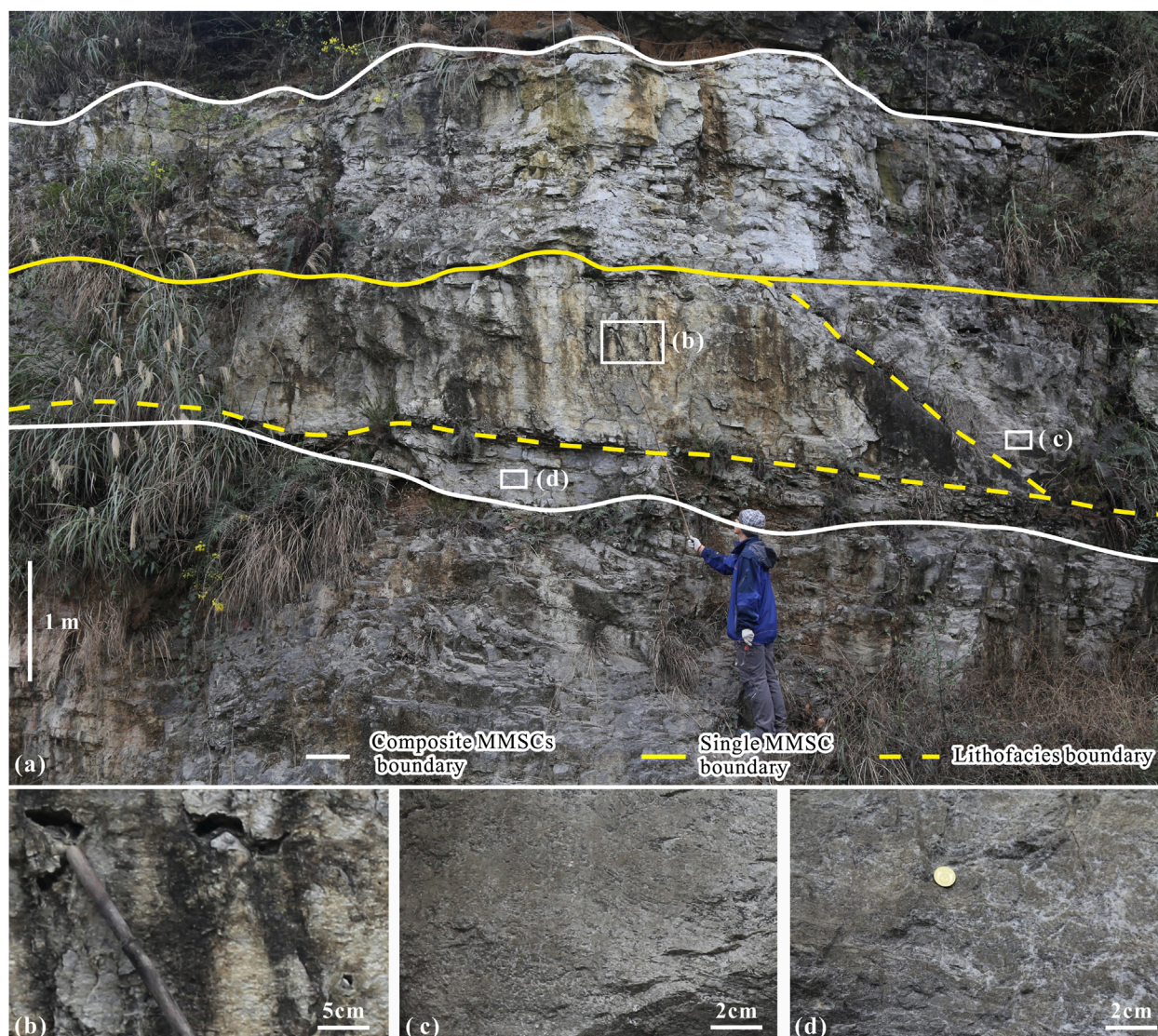


FIGURE 5

Division of sedimentary architectural elements of MMSCs. (A) Macroscopic characteristics of MMSC architectural elements, Xianfeng outcrop, Deng-2 member; (B) thrombolitic dolomite, centimeter-scale caves, mound core; (C) granular dolomite, mound flank; and (D) laminar stromatolitic dolomite, mound flat.

manifests as upward-shallowing sedimentary cycles or indistinct cyclical characteristics. The lower part comprises laminar stromatolitic dolomites, transitioning upward to undulate stromatolitic dolomites. The isolated MMSC exhibits a combination of mound base–mound core–mound cap or mound base–mound core–mound flat.

4.4 Sedimentary evolution characteristics in different outcrops

Given that the Deng-2 and Deng-4 members are the primary intervals for MMSC development, this paper focuses on describing the vertical depositional sequence of three typical outcrops during the sedimentation periods of these two members of the Dengying Formation.

4.4.1 Deng-2 member

4.4.1.1 Xianfeng outcrop

The lower 60 m of the Xianfeng outcrop's Deng-2 member is predominantly characterized by thick-bedded thrombolitic and undulate stromatolitic dolomites, interbedded with granular dolomites (Figure 7), and exhibits well-developed mound cores and mound flanks. The middle 80 m of the outcrop is dominated by thick-bedded thrombolitic dolomites, interlayered with laminar stromatolitic dolomites, indicating deposition of mound cores and featuring minor mound base and mound flat. At the top 80 m of the outcrop, the predominant lithology is micritic dolomites, with a thick sequence of 20 m consisting of undulate and laminar stromatolitic dolomites.

The Xianfeng outcrop Deng-2 member exhibits a three-stage evolution from the carbonate platform margin

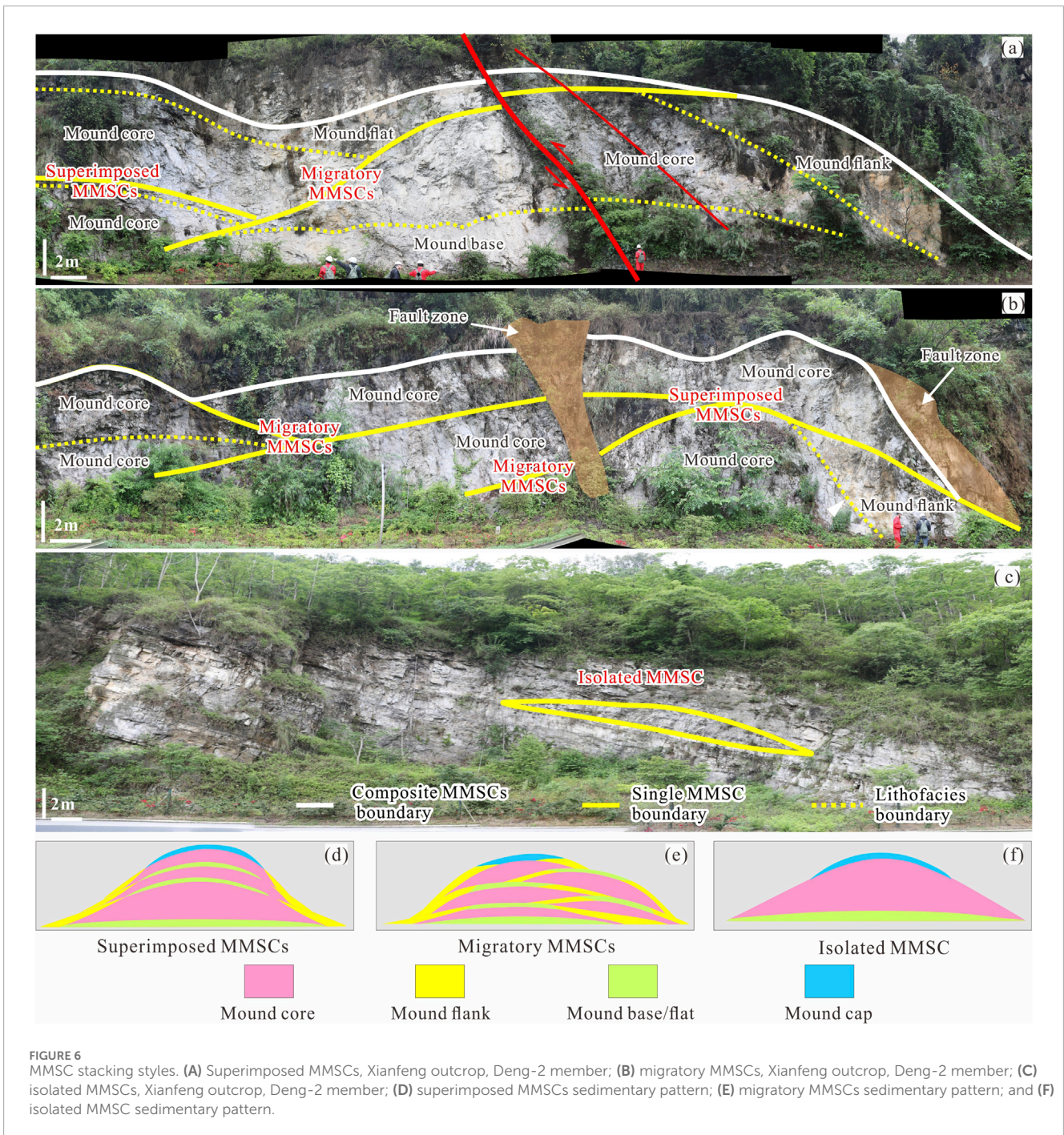
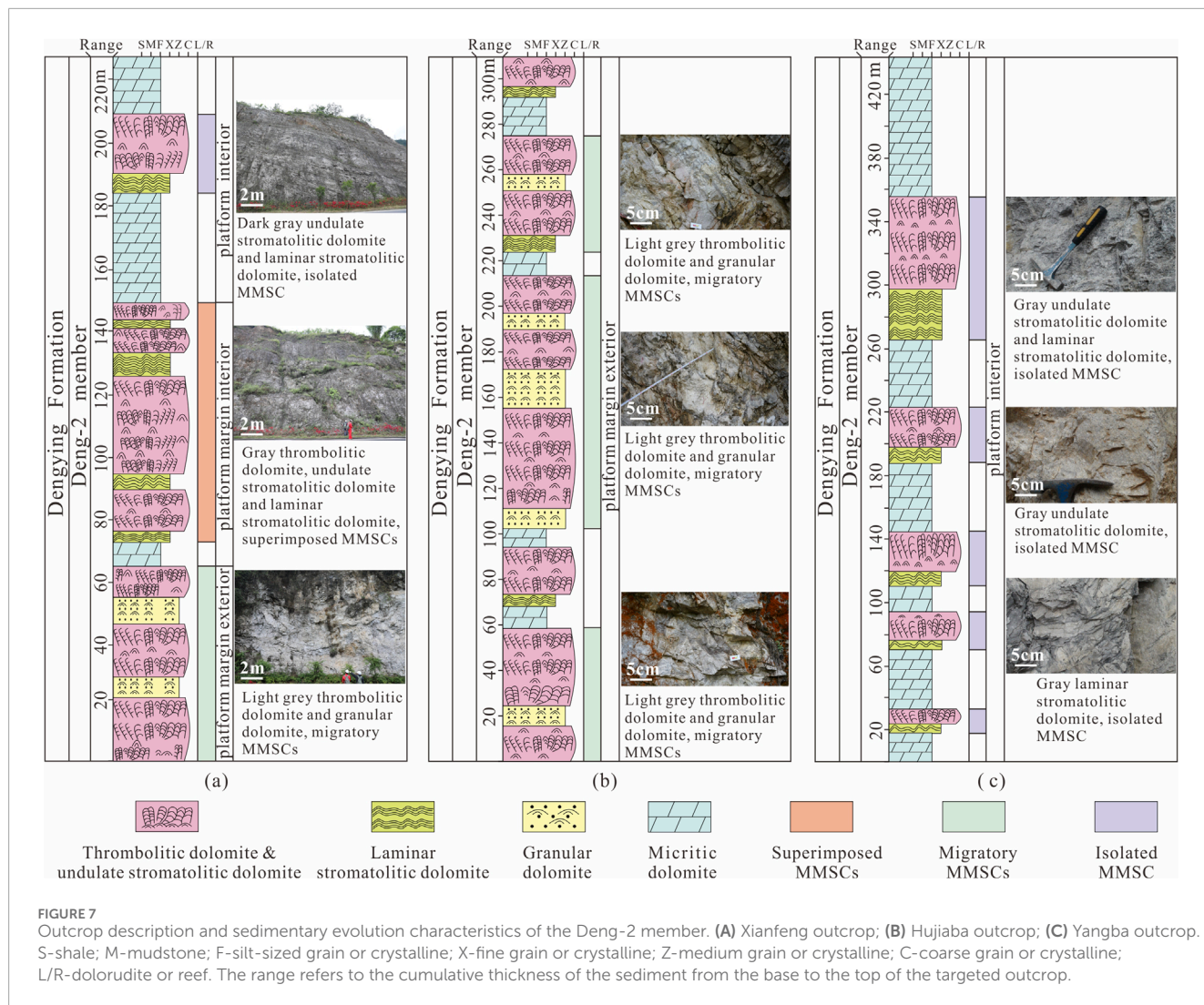


FIGURE 6 MMSC stacking styles. **(A)** Superimposed MMSCs, Xianfeng outcrop, Deng-2 member; **(B)** migratory MMSCs, Xianfeng outcrop, Deng-2 member; **(C)** isolated MMSCs, Xianfeng outcrop, Deng-2 member; **(D)** superimposed MMSCs sedimentary pattern; **(E)** migratory MMSCs sedimentary pattern; and **(F)** isolated MMSC sedimentary pattern.

exterior to the platform interior, characterized by decreasing development and scale of MMSCs and reduced overlap, displaying characteristics of deepening water. The lower 60 m of the outcrop, located on the platform margin exterior, features highly energetic and migratory MMSCs. The middle 80 m of the outcrop, situated on the platform margin interior, shows relatively low hydrodynamic conditions and superimposed MMSCs. The upper 80 m of the outcrop represents the platform interior, where low hydrodynamic, isolated MMSCs are developed.

4.4.1.2 Hujiaba outcrop

Thick-bedded thrombolitic, undulate stromatolitic, and laminated dolomites, interbedded with granular, laminar stromatolitic, and micritic dolomites, characterize the lower portion of the Hujiaba outcrop's Deng-2 member, which is approximately 100-m thick (Figure 7). In the middle of the outcrop, a sequence spanning 160 m exhibits undulate stromatolitic, thrombolitic, and granular dolomites, interspersed with micritic dolomites, collectively indicative of MMSC deposition. The upper 40 m of the outcrop can be divided into two segments: the lower 20 m, which



are predominantly micritic dolomites, and the upper 20 m, which are dominated by thrombolitic dolomites.

The Hujiaba outcrop Deng-2 member is located on the platform margin exterior, featuring high hydrodynamic migratory MMSCs with developed mound cores and mound flanks.

4.4.1.3 Yangba outcrop

The Yangba outcrop exhibits five sets of MMSCs in the Deng-2 member, characterized by distinct inverse cycles (Figure 7). The lower parts of each cycle consist of laminar stromatolitic dolomites, transitioning to undulate stromatolitic dolomites in the upper parts. The five MMSCs increase in size from bottom to top. The lowermost MMSC has a thickness of approximately 15 m, the middle three MMSCs range in thickness from 25 to 35 m, and the uppermost MMSC has a thickness of approximately 90 m.

The Yangba outcrop Deng-2 member is situated within the platform interior, primarily characterized by inter-mound sedimentation dominated by micritic dolomites, featuring isolated MMSCs.

4.4.2 Deng-4 member

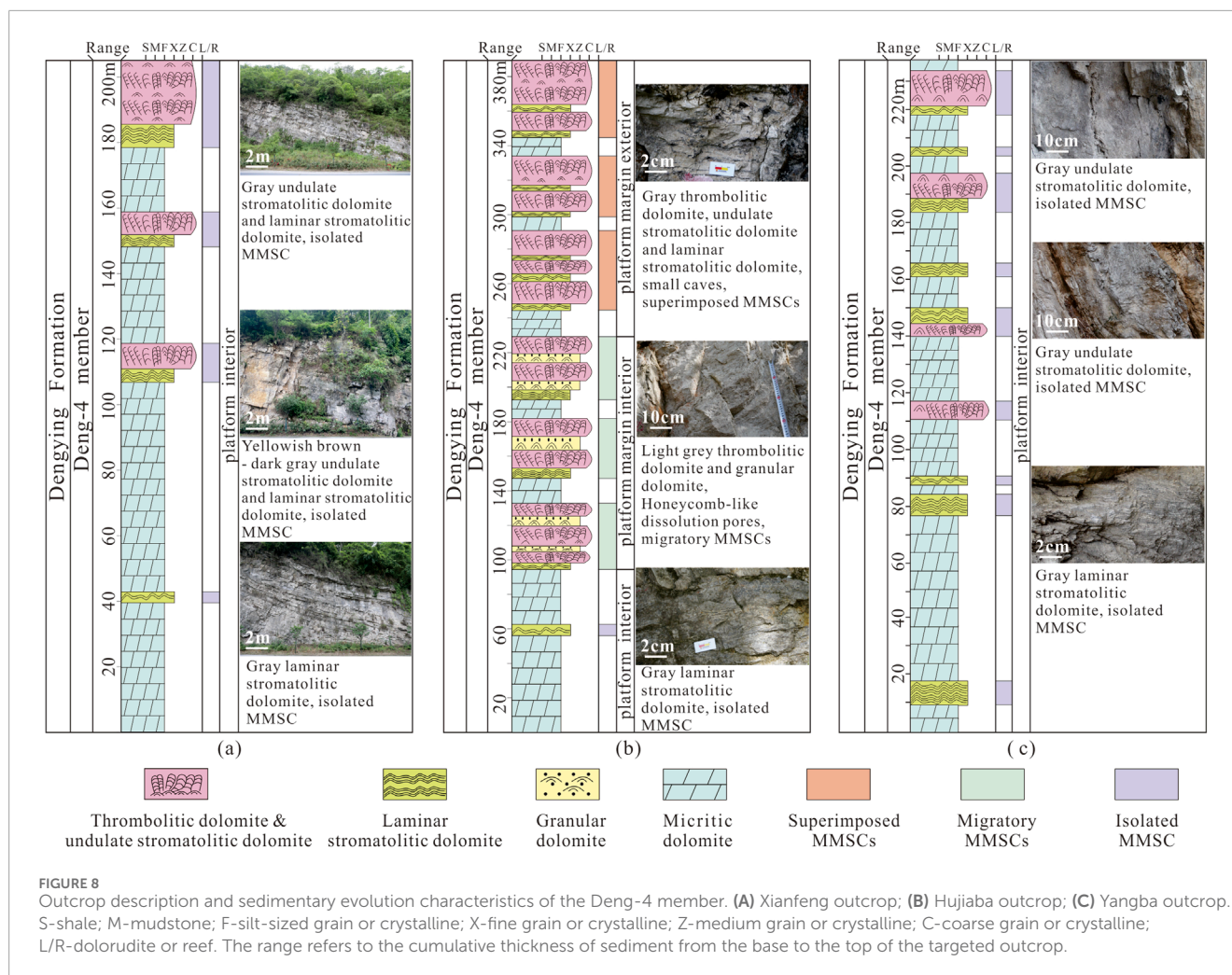
4.4.2.1 Xianfeng outcrop

The Xianfeng outcrop is dominated by micritic dolomites, intercalated with minor occurrences of laminar and undulate stromatolitic dolomites (Figure 8). The lower 100 m of the outcrop consists primarily of thick-bedded micritic dolomites, interbedded with a thin sequence of laminar stromatolitic dolomites. Above this, three sets of MMSCs are developed, with increasing thickness from bottom to top, measuring 10 m, 10 m, and 25 m, respectively. Each MMSC comprises laminar stromatolitic dolomites at the base and undulate stromatolitic dolomites in the upper part, separated by thick-bedded micritic dolomites between the MMSCs.

The Xianfeng outcrop Deng-4 member is situated within the platform interior, primarily characterized by inter-mound sedimentation dominated by micritic dolomites, featuring isolated MMSCs.

4.4.2.2 Hujiaba outcrop

The lower 100 m of the Hujiaba outcrop, Deng-4 Member, comprises micritic dolomites. The middle part, approximately 150-m thick, is characterized by laminar stromatolitic, undulate



stromatolitic, and granular dolomites, with minor interbeds of micritic dolomites (Figure 8). The upper 150 m of the outcrop predominantly consists of thrombolitic and undulate stromatolitic dolomites, interspersed with laminar stromatolitic and micritic dolomites.

The Hujiaba outcrop Deng-4 member exhibits a three-stage evolution from the platform interior to the platform margin exterior, characterized by increasing development and scale of MMSCs and enhanced stacking, displaying characteristics of shallowing water. The lower 100 m of the outcrop, located on the platform interior, features low hydrodynamic, isolated MMSCs. The middle 150 m of the outcrop, situated on the platform margin interior, shows relatively low hydrodynamic conditions and migratory MMSCs. The upper 150 m of the outcrop represents the platform margin exterior, with highly energetic and superimposed MMSCs developed.

4.4.2.3 Yangba outcrop

The Yangba outcrop of the Deng-4 member is predominantly characterized by thick-bedded micritic dolomites, intercalated with minor amounts of laminar and undulate stromatolitic dolomites, averaging approximately 5 m in thickness (Figure 8). At the top, there are two sets of thick-bedded MMSCs, each averaging 10 m in thickness.

The Yangba outcrop Deng-4 member is situated within the platform interior, primarily characterized by inter-mound sedimentation dominated by micritic dolomites, featuring isolated MMSCs.

5 Discussion

5.1 Controlling factors of MMSC stacking styles

This paper uses the Xianfeng outcrop of the Deng-2 member as an example to analyze the controlling factors of different MMSC stacking styles. Previous researchers conducted a study on the sea level variations of the Xianfeng outcrop of the Deng-2 member based on field outcrop sampling, utilizing oxygen-18 isotopes (Luo B. et al., 2013). They identified three stages of sea level changes: a slight rise, a slight fall, and a significant rise, correlating well with the aforementioned lithofacies characteristics and the tripartite sedimentary evolution features. In the early stage of the Deng-2 member, although sea level increased slightly, the sedimentation rate of MMSCs exceeded the rate of accommodation space increase, leading to the development of migratory MMSCs (Figure 9). In

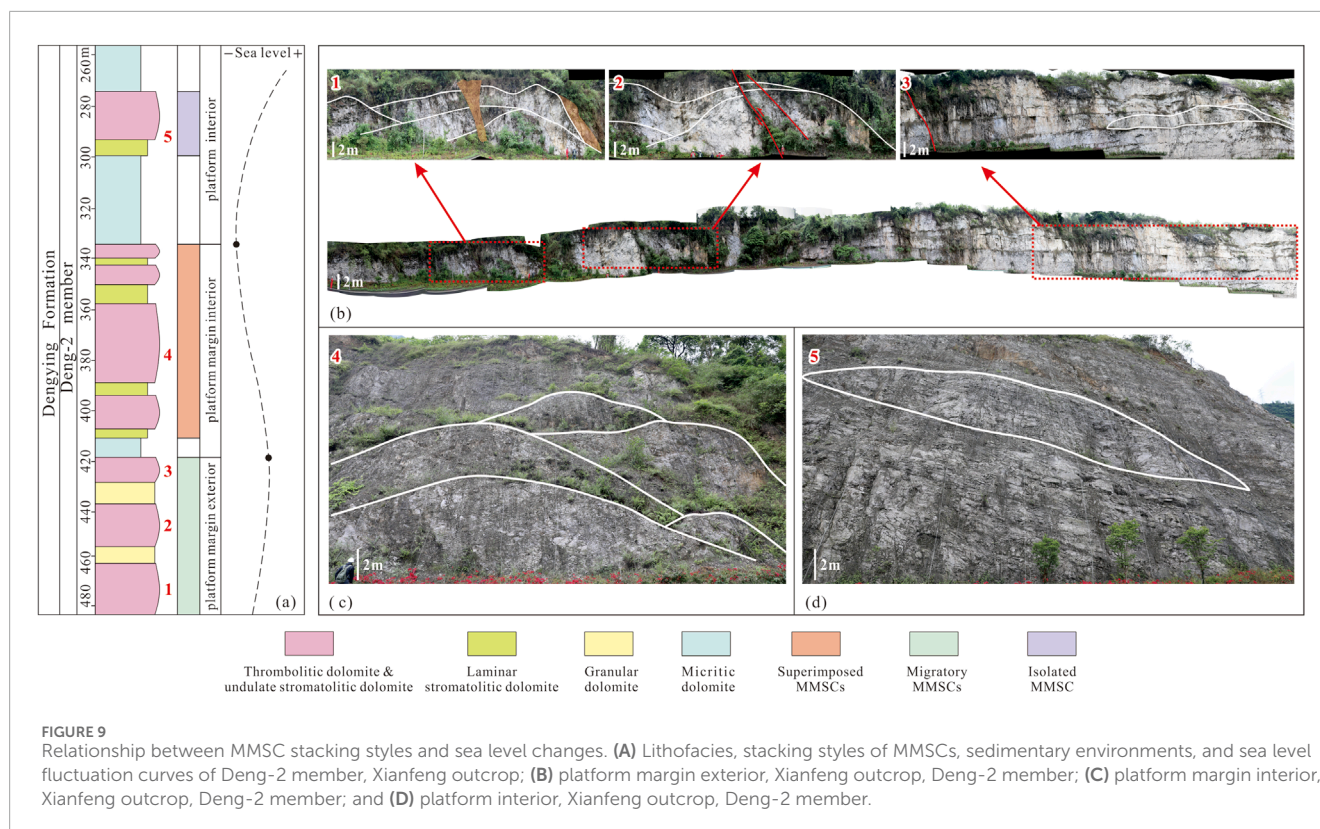


FIGURE 9

Relationship between MMSC stacking styles and sea level changes. (A) Lithofacies, stacking styles of MMSCs, sedimentary environments, and sea level fluctuation curves of Deng-2 member, Xianfeng outcrop; (B) platform margin exterior, Xianfeng outcrop, Deng-2 member; (C) platform margin interior, Xianfeng outcrop, Deng-2 member; and (D) platform interior, Xianfeng outcrop, Deng-2 member.

the middle stage of the Deng-2 member, sea level decreased slightly, with the sedimentation rate of MMSCs approximately equal to the rate of accommodation space reduction, resulting in the development of superimposed MMSCs. In the late stage of the Deng-2 member, sea level increased significantly, with the sedimentation rate of MMSCs less than the rate of accommodation space increase, fostering the development of isolated MMSCs. Therefore, the stacking styles of MMSCs are fundamentally controlled by the relationship between the sedimentation rate of MMSC deposits and the rate of accommodation space variation. During the Deng-2 member, stable carbonate platforms developed, where changes in accommodation space were primarily associated with sea level fluctuations, in the absence of significant tectonic subsidence and relatively stable sedimentary topography. In essence, the stacking styles of MMSCs are mainly influenced by the sedimentation rate of MMSCs and fluctuations in sea level.

The superimposed MMSCs are primarily composed of lithofacies deposited in high hydrodynamic environments, predominantly developed in the platform margin, where sedimentary hydrodynamics are robust. As sea levels gradually rise or fall, the sedimentation rate of MMSCs roughly matches the change rate of accommodation space. Each individual MMSC primarily undergoes vertical accretionary deposition processes, resulting in continuous vertical growth and the formation of thick MMSCs (Figure 10A).

The migratory MMSCs are primarily composed of lithofacies deposited in high hydrodynamic environments, predominantly developed in the platform margin with strong sedimentary hydrodynamics. In relatively elevated topography, the sedimentation rate of the MMSC exceeds the change rate of accommodation

space. After initial deposition on the high topography, a single MMSC migrates to deposit on lower topography with greater accommodation space. Late-stage mound flank occurs above the mound core of early-stage MMSCs, dominated by lateral accretion deposition, resulting in horizontal and vertical growth, forming moderately thick MMSCs (Figures 10B, C).

The isolated MMSC is primarily composed of lithofacies deposited in low hydrodynamic environments, predominantly developed in platform interiors. Platform interior features weak hydrodynamic conditions and limited nutrient availability, resulting in MMSC sedimentation rates lower than the change rate of accommodation space (Figure 10D). In extreme scenarios, sudden deepening of the water halts MMSC growth, leading to reduced thickness.

5.2 Reservoir condition of different architecture elements

Diverse types of MMSCs exhibit differences in dissolution intensity, thus exerting control over porosity and reservoir development.

During the MMSC deposition, frequent exposure due to cyclical sea level fluctuations results in penecontemporaneous dissolution and pores, with varying degrees of dissolution among different MMSC stacking styles (Figure 11). Through the analysis of the dissolution characteristics of different stacking types of MMSCs, it is found that the superimposed MMSC growth rate is essentially consistent with the rate of sea level change. In situations where the sea level frequently fluctuates, they are prone to exposure

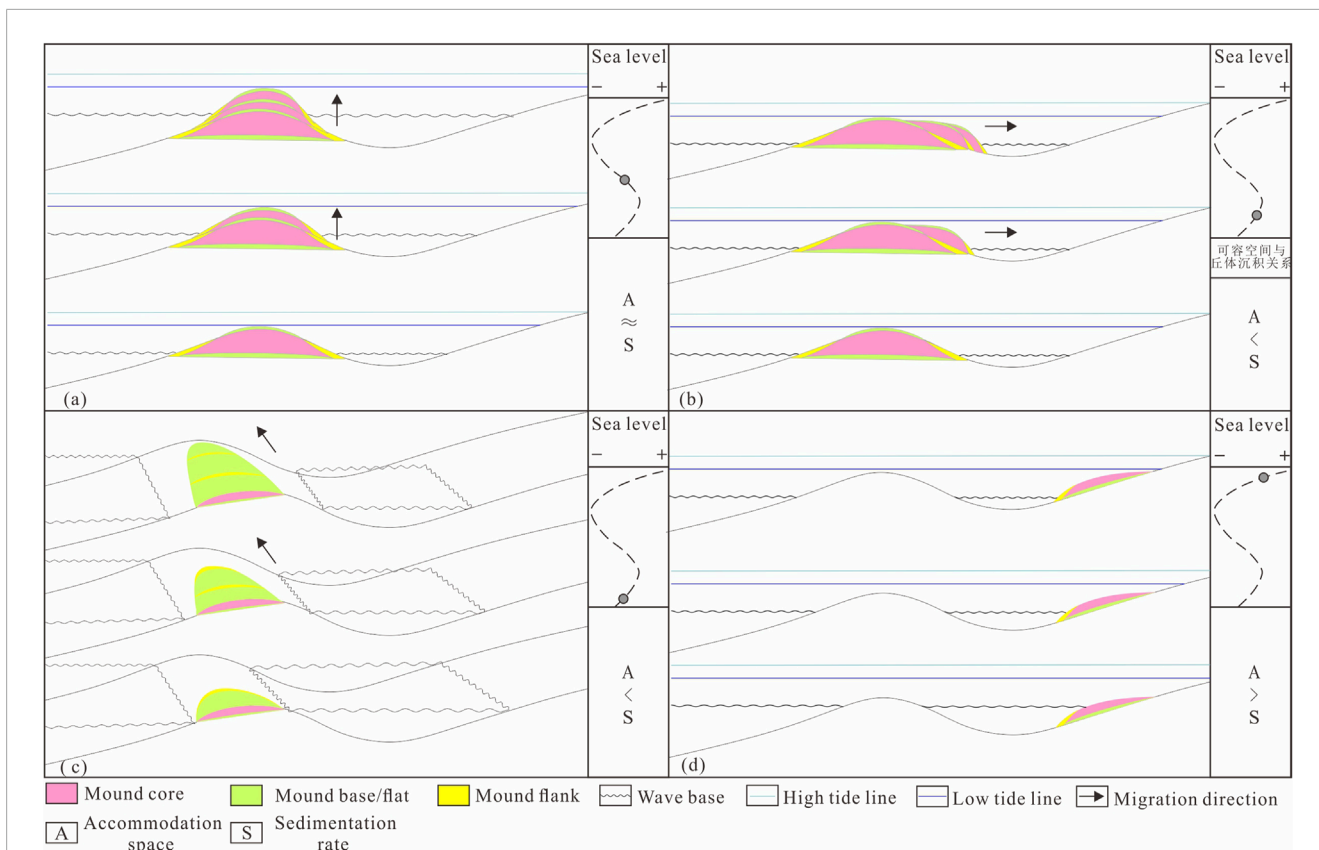


FIGURE 10 Relationship between MMSC stacking styles and sea level changes. **(A)** Superimposed MMSCs, vertical accretion; **(B)** migratory MMSCs, lateral accretion, vertical to the platform margin; **(C)** migratory MMSCs, lateral accretion, parallel to the platform margin; and **(D)** isolated MMSCs.



FIGURE 11 Dissolution differences of different stacking styles of MMSCs. **(A)** Superimposed MMSCs, thrombolitic dolomite, honeycomb-shaped dissolved pores, Deng-4 member, Hujiaba outcrop; **(B)** migratory MMSCs, granular dolomite, needle-like dissolved pores, Deng-4 member, Hujiaba outcrop; and **(C)** isolated MMSCs, laminar stromatolitic dolomite, isolated dissolved pores, Deng-2 member, Xianfeng outcrop.

and susceptible to atmospheric freshwater dissolution, resulting in the highest degree of dissolution. Migratory MMSCs undergo a process of migration and evolution toward low-relief areas with relatively large accommodation spaces. They exhibit poorer exposure and weaker atmospheric freshwater dissolution, with a moderate degree of dissolution intensity. Isolated MMSCs have a slow growth rate and are deposited in deeper water, making them less susceptible to atmospheric freshwater dissolution. They are only briefly exposed during significant sea level drops, resulting in very weak dissolution.

Previous comparative analysis of porosity in different lithologies and depositional facies shows that the average porosity of MMSCs is greater than that of the tidal flat and inter-mound (Zhou et al., 2014; Qin et al., 2015). This study reveals significant variations in porosity among different stacking styles of MMSCs (Figure 12). Based on the results of porosity analysis from field outcrop samples, the average porosity of superimposed MMSCs is 4.9%, the average porosity of migratory MMSCs is 3.2%, and the average porosity of isolated MMSCs is only 2.5%. This is primarily attributed to the stronger hydrodynamic force during the deposition

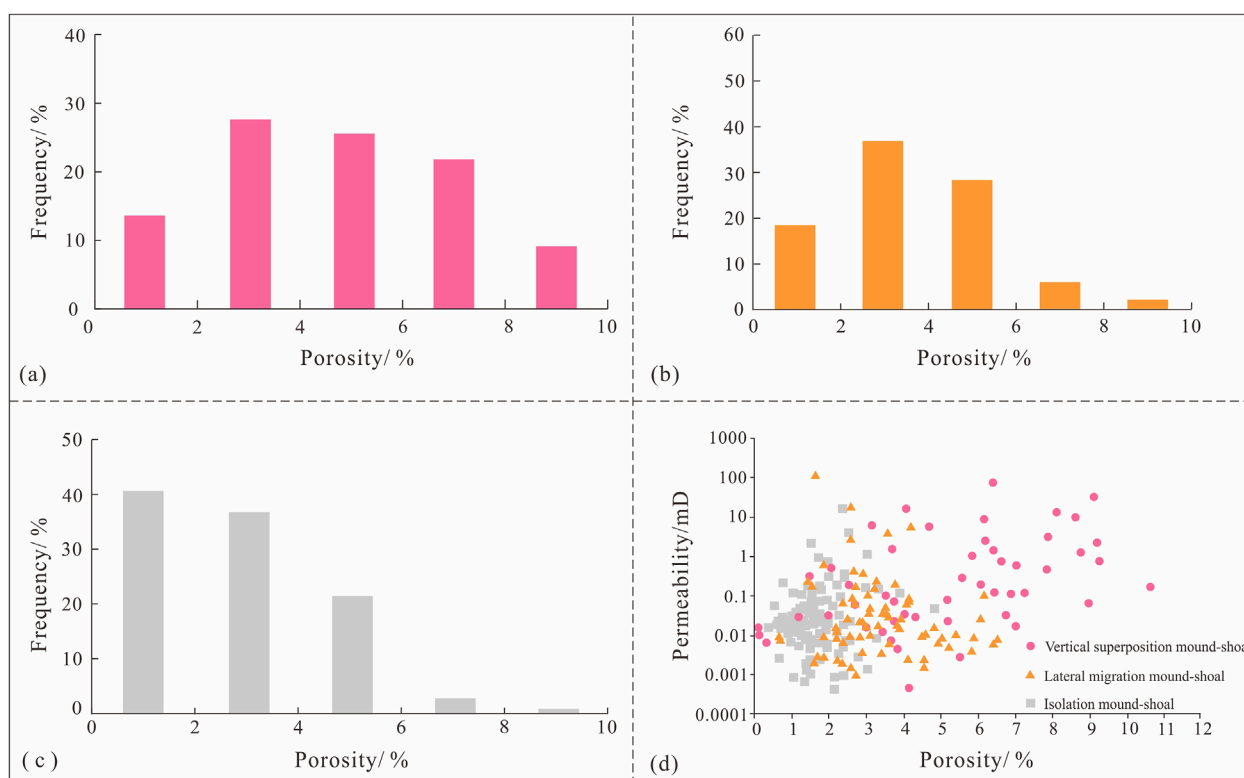


FIGURE 12 Differences in physical properties of MMSCs in different stacking styles. **(A)** Porosity distribution of superimposed MMSCs; **(B)** porosity distribution of migratory MMSCs; **(C)** porosity distribution of isolated MMSCs; and **(D)** porosity and permeability distribution.

of superimposed and migratory MMSCs. Furthermore, porosity variations are also observed within an MMSC (Figure 13). The mound core and mound flank exhibit stronger hydrodynamic conditions, which are more conducive to the development of high-quality reservoirs. Porosity measurements indicate that the mound core and mound flank possess higher porosity values, averaging 5.46% and 4.81%, respectively. In contrast, the mound base and mound cap exhibit lower porosity values, with averages of 2.36% and 1.72%, respectively.

Outcrop petrophysical analysis results typically do not align precisely with subsurface reservoir data. However, in this study area, the reservoir is predominantly controlled by MMSCs. Due to the more complex diagenesis, greater burial depth, and enhanced compaction experienced by subsurface reservoirs, the petrophysical properties of core samples are generally lower than those observed at outcrops. Despite the discrepancies in specific values, the overall trend remains consistent. Whether measured from core samples or outcrop analyses, porosity consistently shows that mound cores and mound flanks exhibit superior properties compared to mound bases and mound flats. This relative variation in petrophysical properties is instructive for understanding the impact of MMSC sedimentary architecture on reservoir characteristics.

Therefore, various composite MMSCs are isolated from each other by sedimentation formed under low hydrodynamic

conditions, constituting distinct connectivity units. Compared to isolated MMSCs, superimposed and migratory MMSCs exhibit superior reservoir condition. Within an individual MMSC, the influence of physical properties in different lithofacies typically results in high-quality reservoirs in mound core and mound flank, whereas mound base, mound flat, and mound cap predominantly form non-reservoir.

6 Conclusion

MMSC primarily develops five lithofacies, namely, thrombolitic dolomite, undulate stromatolitic dolomite, laminar stromatolitic dolomite, granular dolomite, and micritic dolomite. Among these, thrombolitic, undulate stromatolitic, and granular dolomite are products of high hydrodynamic depositional environments, whereas laminar stromatolitic and micritic dolomite are products of low hydrodynamic depositional environments.

The sedimentary architecture of MMSCs is categorized into composite MMSCs, single MMSCs, and lithofacies. Three stacking styles of MMSC are observed: superimposed MMSCs, representing aggradational sedimentation; migratory MMSCs, depicting progradational sedimentation; and isolated MMSCs, denoting a single depositional cycle. The stacking styles of MMSCs are fundamentally controlled by the relationship between MMSC sedimentation rates and variations in accommodation space, with

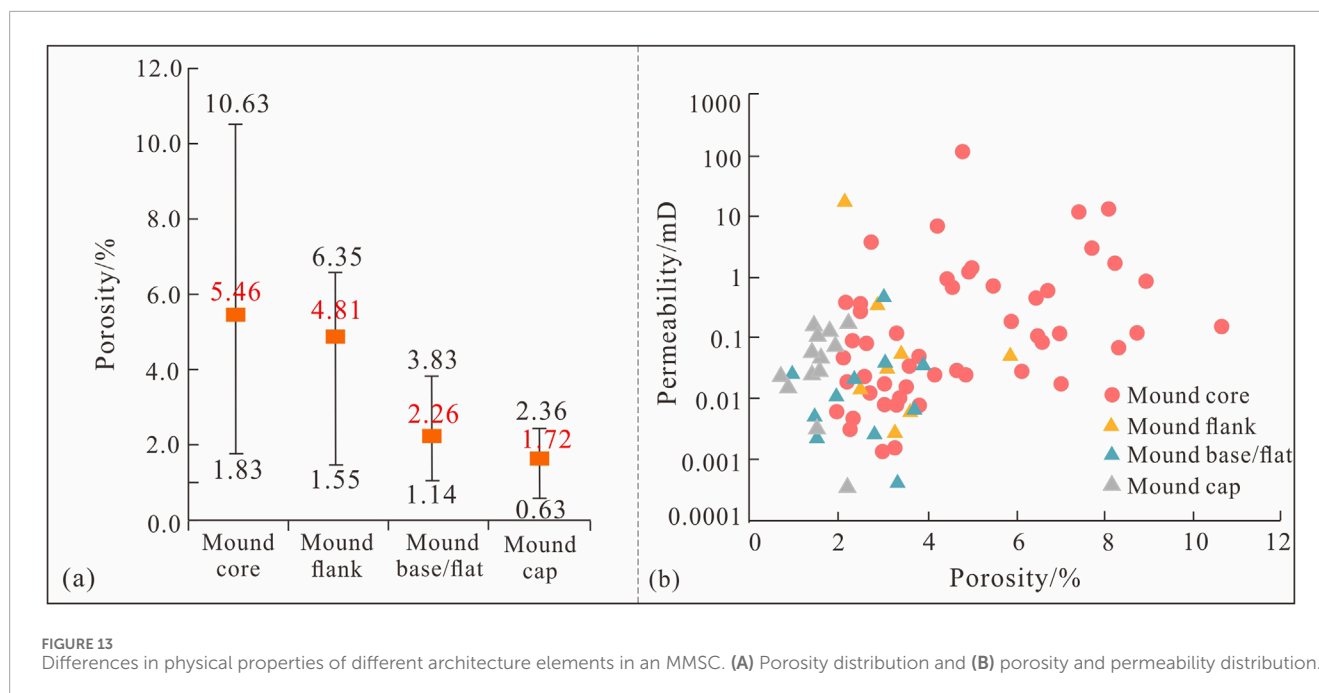


FIGURE 13 Differences in physical properties of different architecture elements in an MMSC. (A) Porosity distribution and (B) porosity and permeability distribution.

sea level fluctuations primarily influencing accommodation space changes. Superimposed MMSC sedimentation rates are comparable to accommodation space change rates, while migratory MMSC sedimentation rates exceed accommodation space change rates, and isolated MMSC sedimentation rates are lower than accommodation space change rates.

Various composite MMSCs are isolated from each other by sedimentation formed under low hydrodynamic conditions, constituting distinct connectivity units. Compared to isolated MMSCs, superimposed and migratory MMSCs exhibit superior reservoir conditions. Within an individual MMSC, different lithofacies lead to high-quality reservoirs in mound cores and flanks due to variations in physical properties, while mound bases, flats, and caps form non-reservoirs.

Data availability statement

The original contributions presented in the study are included in the article/supplementary material; further inquiries can be directed to the corresponding author.

Author contributions

QX: conceptualization, writing—original draft, and writing—review and editing. ZG: funding acquisition and writing—review and editing. FZ: project administration and writing—review and editing. LZ: supervision and writing—review and editing. RX: project administration and writing—review and editing. XW: visualization and writing—review and editing. WL: resources and writing—review and editing. SS: resources and writing—review and editing. HY: software and

writing—review and editing. YL: software and writing—review and editing.

Funding

The author(s) declare that financial support was received for the research, authorship, and/or publication of this article. This research was funded by the China National Petroleum Corporation's "14th Five-Year Plan" forward-looking basic science and technology major projects (grant number 2021DJ15) and Scientific Research and Technology Development Project of China National Petroleum Corporation (grant number 2022KT0905). The funder was not involved in the study design, collection, analysis, interpretation of data, the writing of this article, or the decision to submit it for publication.

Acknowledgments

The authors are thankful to the PetroChina Southwest Oil and Gasfield Company for supplying the studied samples and providing the original geological data. The authors also appreciate the editors and reviewers for providing constructive and careful comments that significantly improved the manuscript.

Conflict of interest

Authors QX, ZG, LZ, XW, WL, SS, HY, and YL were employed by PetroChina. Authors FZ and RX were employed by Southwest Oilfield Company, PetroChina.

Publisher's note

All claims expressed in this article are solely those of the authors and do not necessarily represent those of their affiliated

organizations, or those of the publisher, the editors and the reviewers. Any product that may be evaluated in this article, or claim that may be made by its manufacturer, is not guaranteed or endorsed by the publisher.

References

- Bathurst, R. G. C. (1982). Genesis of stromatolite cavities between submarine crusts in Palaeozoic carbonate mud buildups. *J. Geol. Soc.* 139 (2), 165–181. doi:10.1144/gsjgs.139.2.0165
- Bosence, D. W. J., and Bridges, P. H. (1995). "A review of the origin and evolution of carbonate mud-mounds," in *Carbonate mud-mounds*. Editor C. L. V. Monty, D. W. J. Bosence, and P. H. Bridges 1st ed. (Wiley), 1–9.
- Bridges, P. H., Gutteridge, P., and Pickard, N. A. H. (1995). "The environmental setting of early carboniferous mud-mounds," in *Carbonate mud-mounds*. Editor C. L. V. Monty, D. W. J. Bosence, and P. H. Bridges (Oxford, UK: Blackwell Publishing Ltd.), 171–190.
- Burne, R. V., and Moore, L. S. (1987). Microbialites: organosedimentary deposits of benthic microbial communities. *PALAIOS* 2 (3), 241. doi:10.2307/3514674
- Cai, Z., and Jia, Z. (1995). Architectural studies of unchanneled marine carbonate shoal. *Earth Science-Journal China Univ. Geosciences* 20 (3), 290–298.
- Dalrymple, R. W., and James, N. P. (2010). *Facies models 4*. St. John's: Geological association of Canada.
- Dong, S., Fu, M., Song, R., Guo, H., and Shen, Q. (2023). Diagenesis and reservoir quality of neoproterozoic dolomitized microbialites following multi-stage diagenetic fluid activity: a case study of the sinian dengying formation, China. *Front. Earth Sci.* 11, 1181863. doi:10.3389/feart.2023.1181863
- Howell, J. A., Martinius, A. W., and Good, T. R. (2014). The application of outcrop analogues in geological modelling: a review, present status and future outlook. *Geol. Soc. Lond. Spec. Publ.* 387 (1), 1–25. doi:10.1144/sp387.12
- Khanna, P., Pyrcz, M., Droxler, A. W., Hopson, H. H., Harris, P. M. M., and Lehrmann, D. J. (2020). Implications for controls on upper cambrian microbial build-ups across multiple-scales, mason county, central Texas, USA. *Mar. Petroleum Geol.* 121, 104590. doi:10.1016/j.marpetgeo.2020.104590
- Krause, F. F., Scotese, C. R., Nieto, C., Sayegh, S. G., Hopkins, J. C., and Meyer, R. O. (2004). Paleozoic stromatolites and zebra carbonate mud-mounds: global abundance and paleogeographic distribution. *Geology* 32 (3), 181. doi:10.1130/g20077.1
- Li, W., Jin, T., Wang, G., Song, J., Luo, P. J., and Luo, P. (2013). Microbial carbonates and their significance in the petroleum exploration. *Bull. Geol. Sci. Technol.* 31 (3), 66.
- Luo, B., Wei, G., Yang, W., and Dong, C. (2013). Reconstruction of the late Sinian paleo-ocean environment in Sichuan basin and its geological significance. *Geol. China* 40 (4), 1099–1111.
- Luo, P., Wang, S., Li, P., Song, J., Jin, T., Wang, G., et al. (2013). Review and perspectives of microbial carbonate reservoirs. *Acta Sedimentol. Sin.* 31 (05), 807–823. doi:10.14027/j.cnki.cjxb.2013.05.005
- Mancini, E. A., Benson, D. J., Hart, B. S., Balch, R. S., Parcell, W. C., and Panetta, B. J. (2000). Appleton field case study (eastern Gulf coastal plain): field development model for Upper Jurassic microbial reef reservoirs associated with paleotopographic basement structures (E and P Notes). *AAPG Bull.* 84 (11), 1699–1717. doi:10.1306/8626C36B-173B-11D7-8645000102C1865D
- Mancini, E. A., Llinás, J. C., Parcell, W. C., Aurell, M., Bádenas, B., Leinfelder, R. R., et al. (2004). Upper jurassic thrombolite reservoir play, northeastern gulf of Mexico. *AAPG Bull.* 88 (11), 1573–1602. doi:10.1306/06210404017
- Mancini, E. A., Parcell, W. C., Ahr, W. M., Ramirez, V. O., Llinás, J. C., and Cameron, M. (2008). Upper jurassic updip stratigraphic trap and associated smackover microbial and nearshore carbonate facies, eastern gulf coastal plain. *AAPG Bull.* 92 (4), 417–442. doi:10.1306/11140707076
- Pas, D., Silva, A. C. D., Dhital, M. R., and Boulvain, F. (2011). Sedimentology of a Mid-Late Ordovician carbonate mud-mound complex from the Kathmandu nappe in Central Nepal. *J. Asian Earth Sci.* 42 (3), 452–467. doi:10.1016/j.jseaes.2011.05.008
- Pratt, B. R. (1982). Stromatolitic framework of carbonate mud-mounds. *J. Sediment. Res.* 52. doi:10.1306/212F80FD-2B24-11D7-8648000102C1865D
- Pratt, B. R. (1995). "The origin, biota and evolution of deep-water mud-mounds," in *Carbonate mud-mounds*. Editor C. L. V. Monty, D. W. J. Bosence, and P. H. Bridges 1st ed. (Wiley), 49–123.
- Qin, Z., Liu, Z., and Zhou, J. (2015). Reservoir characteristics and controlling factors of Dengying formation in the Anyue-Moxi area of the central of Sichuan basin. *J. Northeast Petroleum Univ.* 39 (6), 87–94. doi:10.3969/j.issn.2095-4107.2015.06.010
- Reitner, J., Wilmsen, M., and Neuweiler, F. (1995). Cenomanian/Turonian sponge microbialite deep-water hardground community (Liencrees, Northern Spain). *Facies* 22 (1), 203–212. doi:10.1007/bf02536869
- Ren, J., Song, J., Liu, S., Zhao, R., Luo, Z., Li, Z., et al. (2023). Framework and sedimentary model of microbial mound-bank complex in member 2 of Dengying Formation, Sichuan Basin. *Acta Pet. Sin.* 44 (2), 312–328. doi:10.7623/syxb202302007
- Riding, R. (1991). "Classification of microbial carbonates," in *Calcareous algae and stromatolites*. Editor C. Riding (Berlin, Heidelberg: Springer Berlin Heidelberg), 21–51.
- Riding, R. (2002). Structure and composition of organic reefs and carbonate mud mounds: concepts and categories. *Earth-Science Rev.* 58 (1-2), 163–231. doi:10.1016/s0012-8252(01)00089-7
- Riding, R. (2011). "Microbialites, stromatolites, and thrombolites," in *Encyclopedia of geobiology*. Editor J. Reitner, and V. Thiel (Dordrecht: Springer Netherlands), 635–654.
- Schlager, W. (2003). Benthic carbonate factories of the Phanerozoic. *Int. J. Earth Sci.* 92 (4), 445–464. doi:10.1007/s00531-003-0327-x
- Scotese, C. R. (2009). Late proterozoic plate tectonics and palaeogeography: a tale of two supercontinents, rodonia and pannotia. *Geol. Soc. Lond. Spec. Publ.* 326 (1), 67–83. doi:10.1144/sp326.4
- Song, J., Luo, P., Yang, S., Zhai, X., Zhou, G., and Lu, P. (2012). Carbonate rock microbial construction of the lower cambrian Xiaerblak Formation in sugaitblak area, Tarim Basin. *J. Palaeogeogr.* 14 (3), 341–354.
- Song, J. M., Jin, X., Luo, Z., Liu, S. G., Liu, S. B., Ma, X. Z., et al. (2024). Depositional model of the member deng-2 marginal microbial mound-bank complex of the dengying formation in the southwestern sichuan basin, SW China: implications for the ediacaran microbial mound construction and hydrocarbon exploration. *Petroleum Sci.* 21 (2), 806–822. doi:10.1016/j.petsci.2023.12.005
- Tian, X., Peng, H., Wang, Y., Yang, D., Sun, Y., Zhang, X., et al. (2020). Analysis of reservoir difference and controlling factors between the platform margin and the inner area of the fourth member of Sinian Dengying Formation in Anyue Gas Field, central Sichuan. *Nat. Gas. Geosci.* 31 (9), 1225–1238. doi:10.11764/j.issn.1672-1926.2020.04.007
- Tosolini, A. M. P., Wallace, M. W., and Gallagher, S. J. (2012). Shallow water mud-mounds of the early devonian buchan group, East gippsland, Australia. *Sediment. Geol.* 281, 208–221. doi:10.1016/j.sedgeo.2012.09.007
- Tucker, M. E. (1985). Shallow-marine carbonate facies and facies models. *Geol. Soc. Lond. Spec. Publ.* 18 (1), 147–169. doi:10.1144/gsl.sp.1985.018.01.08
- Tull, S. J. (1997). The diversity of hydrocarbon habitat in Russia. *Pet. Geosci.* 3 (4), 315–325. doi:10.1144/petgeo.3.4.315
- Wang, H., Zhou, Q., Zhou, W., Zhang, Y., and He, J. (2021). Carbonate platform reef-shoal reservoir architecture study and characteristic evaluation: a case of S field in Turkmenistan. *Energies* 15 (1), 226. doi:10.3390/en15010226
- Wang, W., Yang, Y., Wen, L., Luo, B., Luo, W., Xia, M., et al. (2016). A study of sedimentary characteristics of microbial carbonate: a case study of the Sinian Dengying Formation in Gaomo area, Sichuan basin. *Geol. China* 43 (1), 306–318.
- Wang, Z., Jiang, H., Chen, Z., Liu, J., Ma, K., Li, W., et al. (2020). Tectonic paleogeography of Late Sinian and its significances for petroleum exploration in the middle-upper Yangtze region, South China. *Petroleum Explor. Dev.* 47 (5), 946–961. doi:10.1016/s1876-3804(20)60108-2
- Wilson, J. L. (1975). *Carbonate facies in geologic history*. New York, NY: Springer New York.
- Xia, M., Zhang, B., Jia, S., Zhao, C., Feng, M., Shang, J., et al. (2024). Retrogradation of carbonate platforms on a rifted margin: the late ediacaran record of the northwestern yangtze craton (SW China). *Front. Earth Sci.* 12, 1401426. doi:10.3389/feart.2024.1401426
- Xia, Q., Ma, X., Guo, Z., Li, W., Jiang, L., Zhang, L., et al. (2023). Distribution characteristics of paleokarst zones and internal reservoirs in the fourth Member of Dengying Formation in Gaoshiti block, central Sichuan Basin. *Acta Pet. Sin.* 44 (8), 1299–1312+1332. doi:10.7623/syxb202308007
- Xia, Q., Yan, H., Xu, W., Lin, Z., Wenjun, L., Hui, D., et al. (2021). Paleokarst microtopography of the Sinian top and its development characteristics in Moxi area, central Sichuan Basin. *Acta Pet. Sin.*, 42 (10), 1299–1336. doi:10.7623/syxb202110004
- Xia, Q., Yan, H., Xu, W., Zhang, L., Li, Q., Luo, W., et al. (2022). Paleo-karst zone and its control on reservoirs in the fourth member of the Sinian Dengying formation in the Moxi area, central Sichuan Basin. *Carbonates Evaporites* 37 (3), 48. doi:10.1007/s13146-022-00788-z

Yang, Y., Wang, W., Wen, L., Luo, B., Zhang, X., Chen, X., et al. (2021). Sedimentary evolution characteristics and large-scale natural gas accumulation pattern of microbial carbonate in the slope area of major paleouplift, the sichuan basin. *Nat. Gas. Ind.* 41 (3), 38–47. doi:10.3787/j.issn.1000-0976.2021.03.005

Zhao, W., Wang, X., Wang, X., Wang, K., and Shen, A. (2022). Stratigraphic sequence re-determination and lithofacies palaeogeographical characteristics of the sinian Dengying Formation in Sichuan Basin. *J. Palaeogeogr.* 24 (5), 852–870. doi:10.7605/gdxb.2022.05.062

Zhou, Z., Wang, X., Xie, L., Mo, J., and Zhang, J. (2014). Reservoir Features and Physical Influences of the Sinian Dengying Formation (Sinian) in Central Sichuan, China. *Nat. Gas. Geosci.* 25 (5), 701–708. doi:10.11764/j.issn.1672-1926.2014.05.0701

Zhou, Z., Wang, X., Yang, X., Wen, L., Wang, W., Zeng, D., et al. (2022). Multi-factor evaluation of deep karst dolomite reservoir based on paleogeomorphological reconstruction, a case study from the 4th member of the dengying formation in the central sichuan basin, China. *Front. Earth Sci.* 10, 930269. doi:10.3389/feart.2022.930269